A multidrug resistant clinical *P. aeruginosa* isolate in the MLST550 clonal complex: uncoupled quorum sensing modulates the interplay of virulence and resistance

Huiluo Cao[a], Tingying Xia[a§], Yanran Li[a§], Zeling Xu[a§], Salim Bougouffa[b], Yat Kei Lo[a], Vladimir B. Bajic[b], Haiwei Luo[c], Patrick C.Y. Woo[d], Aixin Yan[a]*

[a] School of Biological Sciences, The University of Hong Kong, Pokfulam Road, Hong Kong SAR, China

[b] Computational Bioscience Research Center (CBRC), King Abdullah University of Science and Technology (KAUST), Thuwal, Saudi Arabia

[c] School of Life Sciences, The Chinese University of Hong Kong, Sha Tin, Hong Kong SAR, China

[d] Department of Microbiology, Li Ka Shing Faculty of Medicine, The University of Hong Kong, Hong Kong SAR, China

[§]: These authors contributed equally

Running title: Uncoupled QS modulates virulence in MDR *P. aeruginosa*

*Correspondence:

Dr. Aixin Yan,

School of Biological Sciences, The University of Hong Kong

Email: ayan8@hku.hk; Tel: (852) 22990864; Fax: (852) 25599114

Abstract

Pseudomonas aeruginosa is a prevalent and pernicious pathogen equipped with both extraordinary capabilities to infect the host and to develop antimicrobials resistance (AMR). Monitoring the emergence of AMR high risk clones and understanding the interplay of their pathogenicity and antibiotic resistance is of paramount importance to avoid resistance dissemination and to control *P. aeruginosa* infections. In this study, we report the identification of a multidrug resistant (MDR) *P. aeruginosa* strain PA154197 isolated from a blood stream infection in Hong Kong. PA154197 belongs to a distinctive MLST550 clonal complex shared by two international *P. aeruginosa* isolates VW0289 and AUS544. Comparative genome and transcriptome analysis with the reference strain PAO1 led to the identification of a variety of genetic variations in antibiotic resistance genes and the hyper-expression of three multidrug efflux pumps MexAB-OprM, MexEF-OprN, and MexGHI-OpmD in PA154197. Unlike many resistant isolates displaying an attenuated virulence, PA154197 produces a significantly high level of the *P. aeruginosa* major virulence factor pyocyanin (PYO) and displays an uncompromised virulence compared to PAO1. Further analysis revealed that the secondary quorum sensing system Pqs which primarily controls the PYO production is hyper-active in PA154197 independent of the master QS systems Las and Rhl. Together, these investigations disclose a unique, uncoupled QS mediated pathoadaptation mechanism in clinical *P. aeruginosa* which may account for the high pathogenic potentials and antibiotics resistance in the MDR isolate PA154197.

Introduction

Pseudomonas aeruginosa is a ubiquitous Gram-negative pathogen that causes a variety of notorious infections in humans such as ventilator-associated pneumonia, lung infections of cystic fibrosis (CF) patients, burn wound infection, and various sepsis syndromes. It is the second leading cause of hospital-acquired infections and is especially problematic in ICUs, where it is the leading cause of pneumonia among pediatric patients and is responsible for a large number of urinary tract (10% in US and 19% in Europe), blood stream (3% in US and 10% in Europe), eye, ear, nose, and throat infections (1-3). Compounding the burden of these infections is the extraordinary capability of the pathogen to develop antibiotic and multidrug resistance (MDR) even during the course of antibiotics therapy. *P. aeruginosa* is one of the "ESKAPE" (*Enterococcus spp.*, *Staphylococcus aureus*, *Klebsiella spp.*, *Acinetobacter baumannii*, *Pseudomonas aeruginosa*, and *Enterobacter spp*.) organisms which are recognized by the WHO as an alarming threat to the global public heath associated with antimicrobial resistance (AMR). As a consequence, the diseases outcome of the *P. aeruginosa* infections is the complex interplay of the pathogen (its pathogenicity and virulence), hospital environments (antibiotic therapies and the emergence of AMR), and the patient's conditions (host immune responses) (4-6).

P. aeruginosa is genetically equipped with outstanding intrinsic antibiotic resistance machineries. These include the inducible production of the AmpC cephalosporinase, presence of the housekeeping MexAB-OprM multidrug efflux pump, and the limited permeability of its outer membrane caused by low expression and inefficient porin proteins (4, 7, 8). In addition, the pathogen has extraordinary capabilities of developing acquired antibiotic resistance. Mutational overexpression of one of at least four efflux pumps, MexAB-OprM, MexCD-OprJ, MexEF-OprN,

and MexXY-OprM, encoded in the genome of *P. aeruginosa* often plays an important role in acquired resistance and can lead to clinically significant MDR (9, 10). Among them, the MexAB-OprM pump displays the broadest substrates profile and mutational overexpression of this pump can lead to resistance to all β-lactams (except imipenem), (fluoro)quinolones, tetracyclines, and macrolides in clinics. Similar to the MexAB-OprM pump, overexpression of MexXY is frequent (10-30%) among clinical strains and causes decreased susceptibility to aminoglycosides and cefepime. Overexpression of MexEF-OprN and MexCD-OprJ is less frequent in clinical isolates (<5%) and they mainly affect fluoroquinolones resistance (5, 11). In addition to efflux pump overexpression mediated MDR, *P. aeruginosa* also readily develops resistance to specific class of antibiotics through genetic mutations and acquisition of target or drug inactivation genes. These include overexpression of *ampC* caused by mutations in peptidoglycan-recycling genes *ampD*, *dacB*, or *ampR* that causes resistance to noncarbapenem β-lactams; acquisition of aminoglycosides modification enzymes (AMEs) and ribosomal methyltransferase (Rmts) enzymes which are associated with aminoglycosides resistance; mutations in the DNA gyrase (*gyrA* and *gyrB*) and/or topoisomerase IV (*parC* and *parE*) which results in fluoroquinolone resistance, and mutational repression of the OprD porin which leads to resistance to imipenem (12-15).

Regardless of the resistance mechanisms involved, the emergence and prevalence of MDR *P. aeruginosa* strains continue to rise rapidly world-wide. Although the bacterium displays an overall nonclonal epidemic population structure with most isolates represented by single MLST (multilocus sequence typing) genotypes, MDR or XDR (extensively drug-resistant) *P. aeruginosa* isolates display a much lower clonal diversity than the susceptible isolates and recent studies have reported the existence of MDR/XDR global clones disseminated in different hospitals world-wide

(11, 16, 17). Inter-patient spread of antibiotic resistant mutations linked to the transmission of epidemic CF strains is also reported. These clones are denominated as international high-risk clones. Among them, the most recognized successful clones are the high risk MDR clones ST111, ST175, and ST235, and the Liverpool Epidemic Strain (LES) ST146, which is the most epidemic clone among CF patients (11). Further deeper analysis of the molecular details of their resistance development and closely monitoring of the emerging of new international MDR/XDR high risk clones are of paramount importance to avoid the world-wide dissemination of these clones and to control *P. aeruginosa* infections.

In addition to their broad and high level of antibiotic resistance, many MDR clones, especially the three major international high risk clones ST111, ST175, ST235, are found to be associated with a defined set of biological markers which include defective motility (swimming, swarming, and twitching), reduced pigment production (pyocyanin and pyoverdine), reduced in vitro fitness, but enhanced biofilm formation (5, 11). These suggest the presence of a fitness trade-off that compromises the pathogenic potentials and virulence of MDR isolates. Several epidemiological survey and molecular evolutionary studies ascribed these phenotypes to quorum sensing (QS) deficiency in these strains (18-21), which is not unexpected since production of many virulence factors, such as exo-proteases, elastase, rhamnolipids, lectin, pyoverdine, pyocyanin, hydrogen cyanide etc. are primarily regulated by QS systems in *P. aeruginosa*(1). On the other hand, recent studies also reported antibiotic resistant strains displaying enhanced virulence (17, 22-24), such as *P. aeruginosa* strains lacking the *oprD* porin (22), implying that certain MDR clones may develop compensatory mutations allowing them to recover their virulence without affecting the level of resistance.

Recently, we surveyed 84 *P. aeruginosa* clinical strains isolated from various of infections including wound (both superficial and deep), urine, ear, pus, drain fluid, and blood in the Queen Mary Hospital, Hong Kong, and identified an MDR isolate PA154197 from a blood stream infection. PA154197 displays an MDR level and profile comparable to the international high-risk clone ST175. Sequencing its genome reveals that it belongs to a distinctive genotype MLST550 rather than the ST175 clone. The MLST550 genotype is shared by two additional clinical strains in the database: VW0289 and AUS544 which were isolated from the sputum and bronchial lavage of CF patients in The Netherlands and Australia, respectively, suggesting a potential international transmission of this emerging clonal complex. This combined with the extraordinary antibiotic resistance profile of the strain prompt us to use PA154197 as a prototype to conduct comparative genomic and transcriptomic analysis and understand the resistance development and virulence of the MLST550. These studies led to the identification of the adaptive activation of the secondary quorum sensing system Pqs (*Pseudomonas* quinolone system) independent of the primary QS system Las and Rhl which may account for the uncompromised virulence in the MDR strain PA154197. Together, our studies report the emergence of a high-risk clone in clinics and its underlying pathoadapation mechanism mediated by uncoupled QS.

Results

PA154197 displays extraordinary antibiotic resistance

We examined the susceptibility of PA154197 to various classes of antibiotics including the common antipseudomonal drugs aztreonam (ATM), imipenem (IPM), ciprofloxacin (CIP), levofloxacin (LVX), and amikacin (AMK) by measuring their MIC values and compared with that

for PAO1 (Fig. 1A). We found that PA154197 displays resistance to almost all these different classes of antibiotics with a 4-, 16-, 80-, and 160-fold decreases in susceptibility to the common antipseudomonal drugs ATM, IPM, CIP, and LVX, respectively, compared to PAO1. The only two antibiotics it remains susceptible are the aminoglycoside amikacin and the cyclic non-ribosomal polypeptides polymyxin B and E, which meets the XDR criteria (resistance to all but one or two of the eight classes of antipseudomonal drugs) according to Magiorakos et. al (16). To further evaluate its resistance level, we compared the antibiotics susceptibility profile of PA154197 with the three international high-risk clones using the published data (25) and found that PA154197 displays a comparable resistance profile with the high-risk clone ST175 (Fig. 1B), highlighting the high epidemic and risk potential of PA154197.

Sequencing type, phylogenetic position, and genomic islands of PA154197

We then sequenced the genome of PA154197 which resulted in one single circular chromosome with a length of 6,445,239 bp and a GC content of 66.38%. A total number of 5,923 genes are predicted in PA154197 genome which include 5,816 coding gene sequences (CDS), 26 pseudo-genes, 12 rRNA, 65 tRNA and 4 ncRNA (Table 1). Based on PubMLST, PA154197 is assigned to the multilocus sequence typing (MLST) 550, a clonal complex which is currently shared by two additional clinical isolates, VW0289 and AUS544 from the CF patients in the Netherland and Australia, respectively (Fig. 2A), but the complete genome sequences of these two strains are unavailable. PAst analysis revealed that PA154197 belongs to the Serotype O9 (26) (Table 1). Analyzing its accessory genome identified 21 genome islands (GIs) including 3 prophages (Table S1). In addition to hypothetical proteins, a large number of metabolic enzymes such as oxidoreductase, oxygenase and halogenase, as well as the AraC and LysR type transcription

regulators are encoded in these GIs, implying the potential roles of the accessory genome of PA154197 in the adaptation and fitness of the bacterium.

To examine the phylogenetic relationship of PA154197 with other *P. aeruginosa* strains, we constructed a phylogenetic tree based on 140,634 SNPs generated from 150 *P. aeruginosa* genomes which include all publicly-available complete genomes (78 as of October 2017) and representative non-complete genomes. As shown in Fig 2B, PA154197 exhibits a distinct phylogenetic position from other genomes available in the database. This may indicate its unique virulence and pathogenic potentials.

Antibiotic resistance genes and mutational changes therein

Using Resistance Gene Identifiers (RGI), we then identified antibiotic resistance genes in PA154197 against the Comprehensive Antibiotic Resistance Database (CARD)(27), and examined genomic variations including mutations, deletions and indels in these genes with the genome of PAO1 as the reference (Table 2). It was revealed that PA154197 contains a large number of mutations associated with antibiotic resistance genes, including both previously reported genetic variations and those newly identified in PA154197. Several well established mutations include an 8-bp deletion in the *mexT* gene which leads to up-regulation of the MexEF-OprN efflux pump and down-regulation of the OprD porin, and consequently resistance to fluoroquinolones and imipenem; the T105A substitution in AmpC, which causes resistance to non-carbapenem β-lactams (28), and the T83I substitution in the so called quinolone resistance-determining region (QRDR) of GyrA, conferring quinolone resistance. Another genomic variation commonly found to cause resistance in many *P. aeruginosa* isolates is the non-synonymous mutations in the TetR transcriptional regulator NalC which often leads to aztreonam resistance (29). Three non-

179 synonymous mutations, G71-E, E153-Q, S209-R, are identified in the *nalC* gene in PA154197
180 (Table 2).
181
182 New genomic variations that potentially lead to antibiotic resistance is also identified in
183 PA1541197, such as a 6-bp deletion (corresponding to the deletion of E959 and S969) in the C-
184 terminal of GyrA and a E76-*(stop codon) mutation in the *mexR* gene which will lead to pre-
185 mature termination of MexR at E76 and potentially de-repression of the MexAB-OprM major
186 efflux pump, causing multidrug resistance(30). Mutations that potentially de-repress or induce the
187 expression of several other efflux pumps are also identified in the corresponding transcription
188 regulators or the promoter region of the efflux genes. For example, a single point mutation H398R
189 is identified in *parS* gene which regulates the expression of the *mexEF-oprN* efflux pump (31). A
190 5-nucleotides alteration in the promoter region (-1 to -250bp) of the *mexGHI-opmD* operon is
191 present in PA154197 compared with that in PAO1, which may lead to the expression change of
192 the MexGHI-OpmD efflux pump. A complete summary of the identified genomic variations in all
193 the antibiotic resistance genes is provided in Table 2.
194
195 ***Expression of the resistance genes and the functional genome of P. aeruginosa PA154197***
196 To examine the resistance mechanisms of PA154197 especially the expression levels of the
197 resistance genes identified, we performed a comparative transcriptome analysis on PA154197 and
198 the reference strain PAO1 using RNA-seq. Among the 5,543 orthologous genes identified in the
199 two strains using progressiveMauve (32), differential expression of 3,148 genes are observed and
200 their expression levels are compared using DESeq (33) (Fig. 3 and Table S2). Notably, among the
201 genes which display significantly higher expression levels in PA154197 than in PAO1, those

encoding four efflux pumps, such as *mexEF-oprN* (PA2493-PA2495), *mexRAB-oprM* (PA0424-PA0427), *mexGHI-opmD* (PA4205-PA4208), and *mexKJL* (PA3676-PA3678) are observed (Fig. 3), consistent with the MDR profile of PA154197. Genes that confer resistance to specific antibiotics, such as that of *ampC*, *gyrA*, *gyrB*, and *parC*, *parE*, are not differentially expressed in the RNA-Seq analysis, suggesting that over-expression of several multidrug efflux pumps may play a major role in the MDR development in PA154197. COG functional distribution analysis of the differentially expressed genes also reveals the enrichment of efflux pump genes among all the genes which are expressed at a higher level in PA154197 than in PAO1 (Fig S1).

To verify the relative expression levels of these genes in the two strains, we conducted RT-qPCR analysis. As shown in Fig 4B, consistent with the RNA-Seq data, the MexEF-OprN efflux system displayed the most significant higher expression (265-574 fold) in PA154197 than in PAO1, followed by the MexGHI-OpmD (8.5-41.9 fold) and the MexAB-OprM (4.6-11 fold) efflux system. On the other hand, another efflux system which over-expression is associated with aminoglycosides resistance, the MexXY-OprD system, did not show increased relative expression in PA154197 in either RNA-Seq or the RT-qPCR analysis, consistent with the fact that PA154197 remains susceptible to the aminoglycoside antipseudomonal drug amikacin (Fig 1). Overall, an EB efflux assay showed the hyper-efflux activity in PA154197 than in PAO1 (Fig 4C), suggesting that over-expression of the efflux pumps MexEF-OprN, MexAB-OprM, and MexGHI-OpmD may play a major role in conferring MDR in PA154197. RT-qPCR analysis also revealed the decreased expression of another resistance gene *oprD* in PA154197 which serves as the entry portal of imipenem, consistent with the observed imipenem resistance (MIC as 8μg/ml) in this strain.

***Virulence of P. aeruginosa* PA154197**

Our comparative transcriptome analysis also reveals a significantly higher expression of several virulence genes in PA154197 than in PAO1 (Fig 3 and Table S2). These include the type III (*psc* genes) and the type VI (*tss* and *hcp-1* genes) secretion systems, pyocyanin production (*phz* genes), the PQS quorum sensing system (*pqs* genes), and a series of Fe and heme acquisition genes (*fep* and *has* genes). On the other hand, several genes involved in biofilm formation (such as *psl*, *alg*, *lecA*), motility, pili and fimbrial assembly proteins (such as cup genes), and pyoverdine production (*pvd* genes) are expressed at a lower level in PA154197 than in PAO1.

To examine the virulence factors production and the virulence of PA154197, we examined pycyanin (PYO) and pyoverdine production, swimming and swarming motilities, and biofilm formation of PA154197 and compared with that of PAO1. As shown in Fig 5, PA154197 cells display a significantly higher PYO production than PAO1 cells when grown on both LB plate and in LB liquid broth (Fig 5A). In contrast, PA154197 displays reduced pyoverdine production compared to PAO1 (Fig 5B). Consistent with the lower expression of biofilm genes in PA154197 than in PAO1, PA154197 displays a reduced biofilm formation capability as examined by the crystal violet staining (Fig. 5C). In terms of the motility of the bacterium, PA154197 displays a comparable swimming activity with that of PAO1, but a defective swarming motility (Fig. 5D) which is consistent with the lower expression of the pili and fimbria assembly genes in this strain. To evaluate the in vivo virulence of PA154197, we conducted *Caenorhabditis elegans* fast killing and slow killing assays which are established infection models to evaluate the cytotoxicity and pathogenicity of *P. aeruginosa*, respectively(34). We found that the two strains display a comparable cytotoxicity and pathogenicity (virulence) (Fig. 5E) to the *C. elegans* host. Together, these studies indicate that PA154197 over-expresses a subset of virulence factors and does not display a compromised virulence as reported for many other resistant strains.

248

249 ***The Pqs quorum sensing system is activated in PA154197 independent of the primary QS system***

250 ***Las and Rhl***

251 It is known that three hierarchically organized QS systems, Las, Rhl, and Pqs, regulate the

252 production of an arsenal of virulence factors in *P. aeruginosa* with each being primarily associated

253 with the elastase (encoded by *lasB* gene), rhamnolipid (encoded by *rhlA* gene) and pyocyanin

254 (encoded by *phz* genes) production, respectively (35, 36) (Fig 6A). Among them, the Las system

255 proceeds the Rhl and Pqs systems and is the master regulator of the QS circuit. Several previous

256 epidemiological survey and molecular evolutionary studies have identified *lasR* null and mutant

257 variants in clinical isolates and ascribed the attenuated virulence of the isolates to QS deficiency

258 caused by Las inactivation. To investigate the underlying mechanisms of the uncompromised

259 virulence of PA154197, we examined the RNA-Seq transcription levels of the QS systems and

260 their correspondingly regulated genes, especially virulence genes. We found that while expression

261 of the *lasIR* and *rhlIR* in PA154197 is undetectable, expression of the genes encoding the

262 secondary QS system *pqsA-E* is top three significantly expressed (Log_2 RPKM abundance in a

263 range of 4.1 – 5.4) gene operon in PA154197 than in PAO1. Consistently, genes primarily

264 controlled by the Las and Rhl systems, such as *toxA*, *lasB*, *lecA* are expressed in a lower level in

265 PA154197 than in PAO1, whereas genes controlled by Pqs, such as *phZ* genes, *pqsA-E*, and *phnAB*

266 are expressed in a significantly higher level in PA154197 than in PAO1 (Fig 6A and Table S2).

267 RT-qPCR analysis confirmed this observation (Fig 6B). These data suggest that the secondary QS

268 system Pqs is activated and expressed independent of the primary QS systems Las and Rhl in

269 PA154197, which may account for the hyper-production of a subset of virulence factors and

270 consequently its uncompromised virulence.

Discussion

As a successful and ubiquitous pathogen, *P. aeruginosa* is equipped with extraordinary machineries to adapt to the host environments and antibiotic therapies to survive and disseminate. As a result, the disease development caused by *P. aeruginosa* infections is driven by several dynamic factors, including bacterial pathogenesis, selective forces resulting from the antimicrobial interventions, and the fitness costs of resistance development. It is generally recognized that while acquisition of antibiotic resistance mechanisms confers selective advantages in the presence of antimicrobial therapies, expressing and maintenance of the resistance determinants often incurs metabolic costs to the pathogen and consequently compromises its fitness and pathogenicity potentials (5). How *P. aeruginosa* reconciles this scenario and succeeds in the dynamic cycle of infection and dissemination is not known. In this study, we identify and utilize an MDR *P. aeruginosa* isolate PA154197 which displays a comparable MDR profile to the epidemic high-risk clone ST175 but does not exhibits compromised virulence as a paradigm to examine the underlying pathoadaptive mechanisms. Comparative transcriptome and RT-qPCR analysis reveals an uncoordinated, significant activation of the Pqs quorum sensing system and its regulated virulence genes in PA154197 independent of the primary QS Las and Rhl systems, providing a compensatory mechanism for virulence factor production without the activation of the master and primary QS systems Las and Rhl, as well as the hundreds of genes regulated by them. A schematic diagram to illustrate this pathoadaptive mechanism is shown in Fig 7.

Several previous studies reported QS deficiency in antibiotic resistant clinical isolates and attributed the attenuated virulence of the strains to this mechanism, as these mutants are proposed

to be social cheaters that exploit shared QS products without incurring metabolic costs to themselves (18-21). However, majority of these studies were based on comparative genomic analysis to identify mutations in the QS system genes, and the identified variations were mainly found in the master QS regulator LasR, including both *lasR*-null and various *lasR* point mutations. Consistently, the identified strains often display an overall QS-inactivation phenotype, such as decreased production of all the major QS regulated virulence factors including elastase, rhamnolipids, pyoverdine, pyocyanin. Different from these *lasR* defective isolates, PA154197 produces a significantly higher amount of PYO, a major virulence factor secreted by *P. aeruginosa* (37), and other Pqs regulated gene products than PAO1, while a lower level of Las and Rhl regulated virulence factors and genes than in PAO1. This uncoupled activation of Pqs system ensures the production of a major virulence factor PYO with minimal metabolic burden, thus is beneficial to the fitness and virulence of the pathogen. How *P. aeruginosa* achieves this differential activation is not known currently. We compared the promoter regions of the *lasRI*, *rhlRI*, *pqsR*, and *pqsA-E* operons with the corresponding sequences in PAO1, but did not find any nucleotide alternations that may account for the differential activation of *pqs* genes. Comparative genomics analysis revealed a point mutation Q98P in PA154197 LasR which is located at the α5 of the N-3-oxo-dodecanoyl-homoserine lactone binding domain of the protein but the residue is not located in the binding pocket (38). Whether this point mutation leads to differential activation of the Pqs system warrants further investigations. Notably, Las independent activation of a downstream QS system was also reported in a collection of *P. aeruginosa* isolates from CF patients in which half of the *lasR*-null strains were found to retain the RhlR activity (20). Hence, adaptable QS hierarchy which uncouples a downstream QS system from the master regulator LasR may represent an emerging compensatory mechanism that facilitates the fitness, virulence, and persistence of *P.*

317 *aeruginosa* in the host settings.

318

319 With the increasing frequency of detecting the MDR *P. aeruginosa* isolates from various sources,
320 it is recognized that the resistance traits of a strain are often the result of a complex interaction of
321 several cellular processes and no individual mutation or resistance gene is sufficient to confer
322 clinically significant resistance (39, 40). In this study, we identified multiple genetic variations
323 potentially associated with the resistance development in PA154197. These include both
324 machineries which confer resistance to a diverse class of antibiotics and hence causing MDR(4),
325 such as over-expression of multidrug efflux pumps, and genes which mutations result in resistance
326 to specific classes of antibiotics, such as mutations in *ampC* and *gyrA*. Transcriptome and RT-
327 qPCR confirmed the hyper-expression of three multidrug efflux pumps, MexAB, MexEF, and
328 MexGHI in PA154197, but the expression of *ampC* and *gyrA* was found to be in a similar level to
329 that in PAO1. Whether these two genes contribute to the profile and level of resistance exhibited
330 in PA154197 remains further molecular validation. Notably, both the T105A mutation in AmpC
331 and T83I mutation in GyrA are the well characterized genetic variants associated with antibiotic
332 resistance, which have been termed as the PDC-3 type AmpC variant (28) and the quinolone
333 resistance-determining region (QRDR) hotspot mutation, respectively (14). However, these two
334 mutations are also identified in other *P. aeruginosa* isolates we surveyed such as PA150577 which
335 does not display resistance to β-lactams or fluoroquinolones (data not shown). Hence, the observed
336 resistance to antipseudomonal aztreonam (monobactam) and imipenem (carbepenam) in
337 PA154197 may not be due to the T105A mutation in AmpC, and the observed resistance to
338 ciprofloxacin and levofloxacin (fluoroquinolone) may not be due to the T83I mutation in GyrA.
339 In addition, acquiring additional and extended-spectrum β-lactamase on mobile genetic elements

represents another common mechanism of β-lactam resistance in *P.aeruginosa* (41), but no plasmid encoding β-lactamases are identified in PA154197. Indeed, it has been proposed that genetic background of the drug resistant strains influences the epistatic interactions of the various resistant determinants and the resistance readout (42). This highlights the intricacy of the mechanisms that underlie resistance development of MDR strains and our ongoing targeted molecular investigations and evolutionary trajectory analysis may provide mechanistic insight into these processes.

Materials and methods

Minimum inhibitory concentration measurements

MICs were measured following the standard protocol from ASM with slight modification (43). Single fresh colonies of PA154197 and PAO1 were inoculated in Lysogeny broth (LB) overnight at 37°C with 220-rpm agitation. The resulting cell culture was diluted and distributed to the wells of 96-well plate with a final cell density as 5×10^5 CFU/ml. Selected antibiotics were added to the wells with concentration ranging from 0.25 to 128 μg/ml. Plates were incubated at 37 °C for 16-20 h. MIC values were determined as the concentration of antibiotics. Antibiotic susceptibility profiles of the strains indicated are displayed in color scheme with low susceptibility (high MIC values) in red color and high susceptibility (low MIC values) in blue color. The color scheme is constructed using background filling application in the Excel of MS Office.

Genomic DNA extraction

Extraction of the genomic DNA of PA154197 was performed following the description in a

363 previous study (44). Briefly, PA154197 was cultivated in Luria-Bertani (LB) broth overnight with
364 shaking (220 rpm) at 37℃. Bacterial cells were harvested from 1 ml culture via centrifugation at
365 10,000 rpm for 10 minutes. Genomic DNA was extracted using the QIAamp DNA Mini Kit
366 following the manufacturer's instructions (Qiagen, Hilden, Germany). The concentration and
367 quality of genomic DNA was determined by NanoDrop and agarose (0.8%) gel electrophoresis.
368
369 ***Genome sequencing and annotations***
370 Genome sequencing of *P. aeruginosa* PA154197 was conducted on the Illumina NextSeq (300
371 Cycles) PE150 High Output Flow Cell platform in Georgia Genomics Facility at University of
372 Georgia, USA. SPAdes (45) was used to assemble the reads after removal of adapter, primers, and
373 low quality bases using Trimmomatic (46). The initial assembly of PA154197 genome yielded 21
374 contigs. The 21 contigs were aligned against the reference genome of PAO1 and ATCC 27853 and
375 gaps were filled using Sanger sequencing to generate the complete genome sequence of PA154197.
376 Gene calling and annotation were carried out using the National Center for Biotechnology
377 Information (NCBI)'s Prokaryotic Genome Annotation Pipeline 2.0 (PGAP) (47).
378
379 ***Sequence type and phylogenetic analyses***
380 The multiple locus sequence type (MLST) and serotype of PA154197 was predicted based on the
381 PubMLST database (www.pumlst.org) and the *Pseudomonas aeruginosa* serotyper (PAst) tool
382 (26).
383
384 To carry out the phylogenetic analysis, we downloaded all available complete genomes of *P.*
385 *aeruginosa* (one representative per distinct phylogenetic group) from NCBI GenBank (78 genomes

386 by Oct 2017) (Table S3, for reviewers' information only) and selected 72 representative non-
387 complete genomes that are distributed in the 32 phylogenetic groups as defined in the NCBI. Single
388 nucleotide polymorphisms (SNPs) were collected using Parsnp with default parameters (48) and
389 that of PAO1 served as the reference. SNPs were then used to build a maximum likelihood tree in
390 MEGA (49) with the following parameters: Tamura-Nei substitution model, gamma rate
391 distribution among sites, Nearest-Neighbor-Interchange for tree inference options, a bootstrap
392 value 100, and initial tree was generated using the Neighbor Joining method. Variants were called
393 using the Harvest tools (48) and annotated using SnpEff (50).
394
395 ***Identifications of antibiotic resistance genes (ARG) and mutations therein***
396 Resistance Gene Identifiers (RGI) from the Comprehensive Antibiotic Resistance Database
397 (CARD) (27) were used to identify antibiotic resistance genes in PA154197 using "Perfect and
398 Strict hits only" parameter. BLAST of all genes from the present study against the antibiotic
399 resistance gene database of ResFinder (version 2.1) (51) and BLAST against a database of
400 antibiotic resistance genes curated by ourselves based on previous reports (52) were also conducted.
401
402 Variants of all predicted antibiotic resistance genes were collected from the annotation with SnpEff
403 (50) using PAO1 as the reference. SNPs that cause non-synonymous mutations and gaps less than
404 6 bp were also identified and summarized.
405
406 ***RNA-seq***
407 RNA extraction, quality control, and RNA-Seq were performed in PA154197 and the reference
408 strain PAO1 with three biological replicates following our previous descriptions (44). Stranded

libraries for all RNA samples were constructed using Kapa Biosystems RNA library preparation chemistry in Georgia Genomics Facility at University of Georgia.

Orthologous genes between PAO1 and PA154197 were obtained by comparison using *progressiveMauve* with default settings (32) and were employed in the following RNA-seq analysis. RNA-seq reads were pre-processed for quality control using Trimmomatic (46) and were then mapped to the reference genomes of PAO1 and PA154197 respectively, using Stampy (to speed up the alignment process, alignment was initially conducted using BWA-MEM with default parameters (53) then passed to Stampy with the flags --bamkeepgoodreads -M) (54). SAMtools and BamTools were used for format conversions, statistics, and quality assessment and control (55). The Integrative Genomics Viewer was used to visually inspect mapping quality (56). Fragments counting per genomic features (genes) were performed using featureCounts (*featureCounts -R -M -Q 10 -p -P -s 2 -t gene -g locus_tag --largestOverlap*) (57). Reads that mapped with MAPQ scores below 10 were removed. Enforcing a MAPQ score below 10 also excludes multi-mapped reads albeit the percentage of this category is low (data not shown). DESeq was employed to analyze differentially expressed genes. Selective genes with high expression levels in PA154197 were verified using RT-qPCR. Primers used in the present study are listed in Supplementary Table S4.

Motility assays

The assays were performed as previously described with slight modifications(58). (1) Swimming motility. The semi-solid motility plates were prepared by mixing the LB broth with 0.25% (wt/vol)

agarose. Overnight cultures of PAO1 and PA154197 were sub-cultured (1:200 dilution) into LB broth. When OD_{600} reached 0.1-0.2, 2 µl of cell was spotted at the center of a freshly prepared semi-solid swimming plate. The plates dried at room temperature for 1 h and subsequently were incubated at 37^{o}C for 8 h. Swimming motility was evaluated by measuring the diameter of the covered areas. All assays were conducted in triplicates. (2) Swarming motility. The motility plates were prepared by mixing the M8 broth [21.1 mM Na_2HPO_4, 11 mM KH_2PO_4, 42.8 mM NaCl, 9.3 mM NH_4Cl, 1 mM $MgSO_4$, 0.2% glucose, 0.2% casamino acids, pH 6.5] with 0.5% (wt/vol) agarose. 2 µl of sub-cultures of PAO1 and PA154197 (OD600 of 0.1-0.2) as mentioned above was spotted at the center of a pre-dried swarming plate. The plates were incubated at 37^{o}C, and images of the developed swarms were recorded at 16-48 h. All assays were conducted in triplicates.

Pyocyanin production assay

Pyocyanin production was examined according to a protocol described previously with modification (44). 1 ml of the bacterial culture was subject to centrifugation at 13,000 rpm for 5 min. The supernatant was collected and extracted with 600 µl chloroform following vortex for 10 s twice. After centrifugation at 13,000 rpm for 5 min, the chloroform phase was transferred into a clean tube, and subsequently mixed with 0.5 ml 0.2 M HCl followed by gentle shaking to transfer the pyocyanin to the aqueous phase. The concentration of PYO was determined by measuring the absorbance of the aqueous phase at 510 nm.

Biofilm assay

Crystal violet staining method was used to determine biofilm formation of PAO1 and PA154197 with slight modifications (59). Overnight cultures of *P. aeruginosa* cells were inoculated into

454 0.5 ml of LB broth in 5 mL round bottom polypropylene Falcon tubes (final cell density as 0.1)
455 and incubated statically at 37 ºC for 24 or 48 h to allow biofilm formation. After removing the
456 medium, the biofilms formed at the bottom of the tubes were gently washed with phosphate
457 buffered saline (PBS) three times to remove residual planktonic cells. The tubes were then air-
458 dried and stained with 0.1% crystal violet for 15 min at room temperature. After washing the tubes
459 three times with sterile distilled water to remove excess dye molecules, biofilms were dissolved in
460 150 µl of 30% acetic acid and the optical density (OD) was measured at 595 nm using a 96-well
461 plate spectrometer reader. All experiments were performed in triplicates.
462
463 ***Nematode killing assay***
464 To examine the virulence and pathogenesis of PA154197 compared with PAO1, fast and slow
465 killing kinetics of *Caenorhabditis elegans* (*C. elegans*) were performed with slight modification
466 (60). (1) Fast killing assay. Preparation of the killing plates can be divided into two steps. i) 100
467 µL of overnight culture of PA154197 or PAO1 were spread onto 3.5 cm LB agar plates and
468 incubated at 25ºC for 2 days to produce the toxins. ii) Lawn of PA154197 or PAO1 was scraped
469 from LB agar plates containing the toxins completely using a sterile L spreader. *C. elegans* strain
470 N2 were synchronized by isolating eggs from gravid adults and plating eggs on to lawns of *E. coli*
471 OP50 on NGM [0.25% peptone, 0.3% NaCl, 2% agar, 5 µg/ml cholesterol, 1 mM $MgSO_4$, and 25
472 mM KH_2PO_4 (pH 6)] agar plates followed by incubation at 25ºC for 48-52 h to reach the L4 stage.
473 Each fast killing plate was seeded with 20-30 worms. Plates were incubated at 25°C and scored
474 every 4-6 h. A worm was considered to be dead when it no longer responded to touch. (2) Slow
475 killing assay. The procedure was similar as fast killing assay except the preparation of killing plates.
476 For slow killing plates, lawn of PA154197 or PAO1 was not moved away. All experiments were

477 performed in triplicates.

478

479 ***Pyoverdine (PVD) production assay***

480 The siderophore pyoverdine is observed under UV light as a fluorescent zone around the colony
481 (61). Fresh single colonies of PA154197 and PAO1 were inoculated in LB medium overnight at
482 37 °C with 220-rpm agitation. Following diluting overnight culture to 1×10^9 CFU/ml with fresh
483 LB medium, 10 µl cell suspension was then spotted on a LB agar plate. The plate was incubated
484 at 37 °C for 16-20 h. Fluorescent PVD was visualized and imaged under UV light.

485

486 **Efflux activity assay**

487 Efflux activity of PA154197 and PAO1 cells is examined by ethidium bromide accumulation as
488 described previously (62). Overnight cultures of PA154197 and PAO1 cells were diluted 1:100 in
489 fresh LB broth and grown at 37^{o}C until the OD_{600nm} reached 0.5-0.6. The cells were collected by
490 centrifugation at 4,000g for 10 min at 4^{o}C, washed three times with efflux buffer (50 mM
491 potassium phosphate buffer, pH 7.0, containing 5 mM $MgSO_4$), and then resuspended in the same
492 buffer to an $OD_{600\ nm}$ of 0.5. Following incubation at room temperature (25^{o}C) for 3 min in the
493 presence of 25 mM glucose to energize the cells, ethidium bromide (Sigma-Aldrich) was added to
494 a final concentration of 2 µM. The ethidium bromide fluorescence was measured continuously
495 using the Varioskan Flash Multimode Microplate Reader (Thermal Scientific) at Ex/Em
496 wavelengths of 500 nm/580 nm. Higher fluorescence signal indicates lower efflux activity. Assays
497 were performed in triplicates and mean values were used to plot the efflux curve.

498

Acknowledgements

We thank Dr. Karen Yuen (School of Biological Sciences, HKU) for her help to establish the *C. elegans* killing assay. This work is supported by the Hong Kong University Grants Council General Research Fund (17142316, to AY), Seed Funding for Strategic Interdisciplinary Research Scheme (HKU 2017, to AY), and Shenzhen City Knowledge Innovation Plan (JCYJ20160530174441706 to AY).

Author Contributions: HC, AY designed the studies. HC, TX, YL, ZX, YKL, SB, VBB, conducted the experiments. HL provided sequencing service. PW provided clinical strains. HC, TX, YL, ZX, AY wrote the manuscript.

The authors do not have conflict of interests to declare.

513 **References**
514

515 1. Moradali MF, Ghods S, Rehm BH. 2017. *Pseudomonas aeruginosa* lifestyle: a paradigm
516 for adaptation, survival, and persistence. Frontiers in cellular and infection microbiology
517 7:39.
518 2. Breidenstein EB, de la Fuente-Núñez C, Hancock RE. 2011. *Pseudomonas aeruginosa*: all
519 roads lead to resistance. Trends in microbiology 19:419-426.
520 3. Cheng VC, Wong SC, Ho P-L, Yuen K-Y. 2016. Strategic measures for the control of
521 surging antimicrobial resistance in Hong Kong and mainland of China. Emerging microbes
522 & infections 4:e8.
523 4. Poole K. 2011. *Pseudomonas aeruginosa*: resistance to the max. Frontiers in microbiology
524 2:65.
525 5. Geisinger E, Isberg RR. 2017. Interplay between antibiotic resistance and virulence during
526 disease promoted by multidrug-resistant bacteria. The Journal of infectious diseases
527 215:S9-S17.
528 6. Juan C, Peña C, Oliver A. 2017. Host and pathogen biomarkers for severe *Pseudomonas*
529 *aeruginosa* infections. The Journal of infectious diseases 215:S44-S51.
530 7. Lister PD, Wolter DJ, Hanson ND. 2009. Antibacterial-resistant *Pseudomonas aeruginosa*:
531 clinical impact and complex regulation of chromosomally encoded resistance mechanisms.
532 Clinical microbiology reviews 22:582-610.
533 8. Murray JL, Kwon T, Marcotte EM, Whiteley M. 2015. Intrinsic antimicrobial resistance
534 determinants in the superbug *Pseudomonas aeruginosa*. MBio 6:e01603-15.
535 9. Li X-Z, Plésiat P, Nikaido H. 2015. The challenge of efflux-mediated antibiotic resistance
536 in Gram-negative bacteria. Clinical microbiology reviews 28:337-418.
537 10. Sun J, Deng Z, Yan A. 2014. Bacterial multidrug efflux pumps: mechanisms, physiology
538 and pharmacological exploitations. Biochemical and biophysical research communications
539 453:254-267.
540 11. Oliver A, Mulet X, López-Causapé C, Juan C. 2015. The increasing threat of *Pseudomonas*
541 *aeruginosa* high-risk clones. Drug Resistance Updates 21:41-59.
542 12. Quale J, Bratu S, Gupta J, Landman D. 2006. Interplay of efflux system, *ampC*, and *oprD*

543 expression in carbapenem resistance of *Pseudomonas aeruginosa* clinical isolates.
544 Antimicrobial agents and chemotherapy 50:1633-1641.
545 13. Poole K. 2005. Aminoglycoside resistance in *Pseudomonas aeruginosa*. Antimicrobial
546 agents and Chemotherapy 49:479-487.
547 14. Akasaka T, Tanaka M, Yamaguchi A, Sato K. 2001. Type II topoisomerase mutations in
548 fluoroquinolone-resistant clinical strains of *Pseudomonas aeruginosa* isolated in 1998 and
549 1999: role of target enzyme in mechanism of fluoroquinolone resistance. Antimicrobial
550 agents and chemotherapy 45:2263-2268.
551 15. Köhler T, Michea-Hamzehpour M, Epp SF, Pechere J-C. 1999. Carbapenem activities
552 against *Pseudomonas aeruginosa*: respective contributions of OprD and efflux systems.
553 Antimicrobial agents and chemotherapy 43:424-427.
554 16. Magiorakos AP, Srinivasan A, Carey R, Carmeli Y, Falagas M, Giske C, Harbarth S,
555 Hindler J, Kahlmeter G, Olsson-Liljequist B. 2012. Multidrug-resistant, extensively drug-
556 resistant and pandrug-resistant bacteria: an international expert proposal for interim
557 standard definitions for acquired resistance. Clinical microbiology and infection 18:268-
558 281.
559 17. Gómez-Zorrilla S, Juan C, Cabot G, Camoez M, Tubau F, Oliver A, Dominguez MA, Ariza
560 J, Peña C. 2016. Impact of multidrug resistance on the pathogenicity of Pseudomonas
561 aeruginosa: in vitro and in vivo studies. International journal of antimicrobial agents
562 47:368-374.
563 18. Wang K, Chen Y-q, Salido MM, Kohli GS, Kong J-l, Liang H-j, Yao Z-t, Xie Y-t, Wu H-
564 y, Cai S-q. 2017. The rapid *in vivo* evolution of *Pseudomonas aeruginosa* in ventilator-
565 associated pneumonia patients leads to attenuated virulence. Open biology 7:170029.
566 19. Köhler T, Buckling A, Van Delden C. 2009. Cooperation and virulence of clinical
567 *Pseudomonas aeruginosa* populations. Proceedings of the National Academy of Sciences
568 106:6339-6344.
569 20. Feltner JB, Wolter DJ, Pope CE, Groleau M-C, Smalley NE, Greenberg EP, Mayer-
570 Hamblett N, Burns J, Déziel E, Hoffman LR. 2016. LasR variant cystic fibrosis isolates
571 reveal an adaptable quorum-sensing hierarchy in *Pseudomonas aeruginosa*. MBio
572 7:e01513-16.

21. Köhler T, Guanella R, Carlet J, Van Delden C. 2010. Quorum sensing-dependent virulence during *Pseudomonas aeruginosa* colonisation and pneumonia in mechanically ventilated patients. Thorax 65:703-710.

22. Skurnik D, Roux D, Cattoir V, Danilchanka O, Lu X, Yoder-Himes DR, Han K, Guillard T, Jiang D, Gaultier C. 2013. Enhanced in vivo fitness of carbapenem-resistant *oprD* mutants of *Pseudomonas aeruginosa* revealed through high-throughput sequencing. Proceedings of the National Academy of Sciences 110:20747-20752.

23. Roux D, Danilchanka O, Guillard T, Cattoir V, Aschard H, Fu Y, Angoulvant F, Messika J, Ricard J-D, Mekalanos JJ, Lory S, Pier GB, Skurnik D. 2015. Fitness cost of antibiotic susceptibility during bacterial infection. Science Translational Medicine 7:297ra114-297ra114.

24. Balasubramanian D, Kumari H, Mathee K. 2015. *Pseudomonas aeruginosa* AmpR: an acute–chronic switch regulator. Pathogens and Disease 73:1-14.

25. Cabot G, Ocampo-Sosa AA, Domínguez MA, Gago JF, Juan C, Tubau F, Rodríguez C, Moyà B, Peña C, Martínez-Martínez L, Oliver A. 2012. Genetic Markers of Widespread Extensively Drug-Resistant *Pseudomonas aeruginosa* High-Risk Clones. Antimicrobial Agents and Chemotherapy 56:6349-6357.

26. Thrane SW, Taylor VL, Lund O, Lam JS, Jelsbak L. 2016. Application of WGS data for O-specific antigen analysis and *in silico* serotyping of *Pseudomonas aeruginosa* isolates. Journal of Clinical Microbiology doi:10.1128/jcm.00349-16.

27. Jia B, Raphenya AR, Alcock B, Waglechner N, Guo P, Tsang KK, Lago BA, Dave BM, Pereira S, Sharma AN, Doshi S, Courtot M, Lo R, Williams LE, Frye JG, Elsayegh T, Sardar D, Westman EL, Pawlowski AC, Johnson TA, Brinkman FSL, Wright GD, McArthur AG. 2017. CARD 2017: expansion and model-centric curation of the comprehensive antibiotic resistance database. Nucleic Acids Research 45:D566-D573.

28. Berrazeg M, Jeannot K, Ntsogo Enguéné VY, Broutin I, Loeffert S, Fournier D, Plésiat P. 2015. Mutations in ß-Lactamase AmpC Increase Resistance of *Pseudomonas aeruginosa* Isolates to Antipseudomonal Cephalosporins. Antimicrobial Agents and Chemotherapy doi:10.1128/aac.00825-15.

29. Braz VS, Furlan JPR, Fernandes AFT, Stehling EG. 2016. Mutations in NalC induce

MexAB-OprM overexpression resulting in high level of aztreonam resistance in environmental isolates of *Pseudomonas aeruginosa*. FEMS Microbiology Letters 363:fnw166-fnw166.

30. Choudhury D, Ghosh A, Dhar Chanda D, Das Talukdar A, Dutta Choudhury M, Paul D, Maurya AP, Chakravorty A, Bhattacharjee A. 2016. Premature Termination of MexR Leads to Overexpression of MexAB-OprM Efflux Pump in *Pseudomonas aeruginosa* in a Tertiary Referral Hospital in India. PLOS ONE 11:e0149156.

31. Wang D, Seeve C, Pierson LS, Pierson EA. 2013. Transcriptome profiling reveals links between ParS/ParR, MexEF-OprN, and quorum sensing in the regulation of adaptation and virulence in *Pseudomonas aeruginosa*. BMC Genomics 14:618.

32. Darling AE, Mau B, Perna NT. 2010. progressiveMauve: Multiple Genome Alignment with Gene Gain, Loss and Rearrangement. PLOS ONE 5:e11147.

33. Anders S, Huber W. 2010. Differential expression analysis for sequence count data. Genome Biology 11:R106.

34. Tan M-W, Rahme LG, Sternberg JA, Tompkins RG, Ausubel FM. 1999. *Pseudomonas aeruginosa* killing of *Caenorhabditis elegans* used to identify *P. aeruginosa* virulence factors. Proceedings of the National Academy of Sciences 96:2408-2413.

35. Nadal Jimenez P, Koch G, Thompson JA, Xavier KB, Cool RH, Quax WJ. 2012. The Multiple Signaling Systems Regulating Virulence in *Pseudomonas aeruginosa*. Microbiology and Molecular Biology Reviews 76:46-65.

36. Welsh MA, Blackwell HE. 2016. Chemical probes of quorum sensing: from compound development to biological discovery. FEMS Microbiology Reviews 40:774-794.

37. Pierson LS, Pierson EA. 2010. Metabolism and function of phenazines in bacteria: impacts on the behavior of bacteria in the environment and biotechnological processes. Applied Microbiology and Biotechnology 86:1659-1670.

38. Zou Y, Nair SK. 2009. Molecular Basis for the Recognition of Structurally Distinct Autoinducer Mimics by the *Pseudomonas aeruginosa* LasR Quorum-Sensing Signaling Receptor. Chemistry & Biology 16:961-970.

39. Feng Y, Jonker MJ, Moustakas I, Brul S, ter Kuile BH. 2016. Dynamics of mutations during development of resistance by *Pseudomonas aeruginosa* against five antibiotics.

633 Antimicrobial Agents and Chemotherapy doi:10.1128/aac.00434-16.
634 40. Jochumsen N, Marvig RL, Damkiær S, Jensen RL, Paulander W, Molin S, Jelsbak L,
635 Folkesson A. 2016. The evolution of antimicrobial peptide resistance in *Pseudomonas*
636 *aeruginosa* is shaped by strong epistatic interactions. Nature Communications 7:13002.
637 41. Zhao W-H, Hu Z-Q. 2013. Epidemiology and genetics of CTX-M extended-spectrum β-
638 lactamases in Gram-negative bacteria. Critical Reviews in Microbiology 39:79-101.
639 42. Vogwill T, Kojadinovic M, MacLean RC. 2016. Epistasis between antibiotic resistance
640 mutations and genetic background shape the fitness effect of resistance across species of
641 *Pseudomonas*. Proceedings of the Royal Society B: Biological Sciences 283.
642 43. Lalitha MK. 2004. Manual on Antimicrobial Susceptibility Testing Performance standards
643 for antimicrobial testing: Twelfth Informational Supplement 56238:3.
644 44. Cao H, Lai Y, Bougouffa S, Xu Z, Yan A. 2017. Comparative genome and transcriptome
645 analysis reveals distinctive surface characteristics and unique physiological potentials of
646 *Pseudomonas aeruginosa* ATCC 27853. BMC Genomics 18:459.
647 45. Bankevich A, Nurk S, Antipov D, Gurevich AA, Dvorkin M, Kulikov AS, Lesin VM,
648 Nikolenko SI, Pham S, Prjibelski AD, Pyshkin AV, Sirotkin AV, Vyahhi N, Tesler G,
649 Alekseyev MA, Pevzner PA. 2012. SPAdes: A New Genome Assembly Algorithm and Its
650 Applications to Single-Cell Sequencing. Journal of Computational Biology 19:455-477.
651 46. Bolger AM, Lohse M, Usadel B. 2014. Trimmomatic: a flexible trimmer for Illumina
652 sequence data. Bioinformatics 30:2114-2120.
653 47. Angiuoli SV, Gussman A, Klimke W, Cochrane G, Field D, Garrity GM, Kodira CD,
654 Kyrpides N, Madupu R, Markowitz V, Tatusova T, Thomson N, White O. 2008. Toward
655 an Online Repository of Standard Operating Procedures (SOPs) for (Meta)genomic
656 Annotation. OMICS: A Journal of Integrative Biology 12:137-141.
657 48. Treangen TJ, Ondov BD, Koren S, Phillippy AM. 2014. The Harvest suite for rapid core-
658 genome alignment and visualization of thousands of intraspecific microbial genomes.
659 Genome Biology 15:524.
660 49. Tamura K, Stecher G, Peterson D, Filipski A, Kumar S. 2013. MEGA6: Molecular
661 Evolutionary Genetics Analysis Version 6.0. Molecular Biology and Evolution 30:2725-
662 2729.

663 50. Cingolani P, Platts A, Wang LL, Coon M, Nguyen T, Wang L, Land SJ, Lu X, Ruden DM.
664 2012. A program for annotating and predicting the effects of single nucleotide
665 polymorphisms, SnpEff. Fly 6:80-92.
666 51. Zankari E, Hasman H, Cosentino S, Vestergaard M, Rasmussen S, Lund O, Aarestrup FM,
667 Larsen MV. 2012. Identification of acquired antimicrobial resistance genes. Journal of
668 Antimicrobial Chemotherapy 67:2640-2644.
669 52. Sherrard LJ, Tai AS, Wee BA, Ramsay KA, Kidd TJ, Ben Zakour NL, Whiley DM,
670 Beatson SA, Bell SC. 2017. Within-host whole genome analysis of an antibiotic resistant
671 *Pseudomonas aeruginosa* strain sub-type in cystic fibrosis. PLOS ONE 12:e0172179.
672 53. Li H. 2013. Aligning sequence reads, clone sequences and assembly contigs with BWA-
673 MEM. arXiv preprint arXiv 1303.3997.
674 54. Lunter G, Goodson M. 2011. Stampy: A statistical algorithm for sensitive and fast mapping
675 of Illumina sequence reads. Genome Research 21:936-939.
676 55. Barnett DW, Garrison EK, Quinlan AR, Strömberg MP, Marth GT. 2011. BamTools: a
677 C++ API and toolkit for analyzing and managing BAM files. Bioinformatics 27:1691-1692.
678 56. Thorvaldsdóttir H, Robinson JT, Mesirov JP. 2013. Integrative Genomics Viewer (IGV):
679 high-performance genomics data visualization and exploration. Briefings in
680 Bioinformatics 14:178-192.
681 57. Liao Y, Smyth GK, Shi W. 2014. featureCounts: an efficient general purpose program for
682 assigning sequence reads to genomic features. Bioinformatics 30:923-930.
683 58. Ha D-G, Kuchma SL, O'Toole GA. 2014. Plate-Based Assay for Swimming Motility in
684 *Pseudomonas aeruginosa*, p 59-65. *In* Filloux A, Ramos J-L (ed), Pseudomonas Methods
685 and Protocols doi:10.1007/978-1-4939-0473-0_7. Springer New York, New York, NY.
686 59. Au - O'Toole GA. 2011. Microtiter Dish Biofilm Formation Assay. JoVE
687 doi:doi:10.3791/2437:e2437.
688 60. Kirienko NV, Cezairliyan BO, Ausubel FM, Powell JR. 2014. *Pseudomonas aeruginosa*
689 PA14 Pathogenesis in *Caenorhabditis elegans*, p 653-669. *In* Filloux A, Ramos J-L (ed),
690 Pseudomonas Methods and Protocols doi:10.1007/978-1-4939-0473-0_50. Springer New
691 York, New York, NY.
692 61. Yu X, Chen M, Jiang Z, Hu Y, Xie Z. 2014. The two-component regulators GacS and

693 GacA positively regulate a nonfluorescent siderophore through the Gac/Rsm signaling
694 cascade in high-siderophore-yielding *Pseudomonas* sp. HYS. Journal of Bacteriology
695 doi:10.1128/jb.01756-14.
696 62. Du D, Wang Z, James NR, Voss JE, Klimont E, Ohene-Agyei T, Venter H, Chiu W, Luisi
697 BF. 2014. Structure of the AcrAB–TolC multidrug efflux pump. Nature 509:512.

698

699

700 **Figures legends:**

701 **Figure 1.** Antibiotic resistance profiles of PA154197. **A.** MIC values of various antibiotics to
702 PA154197 and PAO1. **B.** MIC values of indicated antibiotics to the international high risk clone
703 ST175 are retrieved from published data (25) and are compared with that of PA154197. Resistance
704 levels are displayed in color scheme with low susceptibility (high MIC values) in red color and
705 high susceptibility (low MIC values) in blue color. The color scheme is constructed using
706 background filling application in the Excel of Microsoft Office.

707 **Figure 2.** Lineage complex of the MLST550 and phylogenetic position of PA154197. **A.**
708 Geographical distribution of the three MLST550 *P. aeruginosa* strains currently available in
709 pubMLST database, VW0289, VW0289, and PA154197. **B**. phylogenetic relationships of
710 PA154197 with 149 *P. aeruginosa* strains including 78 complete and 71 incomplete genomes from
711 representative 32 groups available in Genbank database (as of October 2017). The phylogenetic
712 tree was constructed based on the SNPs identified using Harvest with 100 bootstrap and maximum
713 likelihood (ML) criterion in MEGA 7 software. Scale bar indicates the branch length and circles
714 on the nodes represent the statistical supports according to size. The denotation of the strain is
715 listed in the Table S3 and PA15419 is highlighted in red.

716 **Figure 3.** The genome wide transcriptomic profile of *P. aeruginosa* PA154197 and PAO1. Orange
717 dots indicate genes with higher relative expression levels in PA154197 than in PAO1 and blue
718 dots represent genes with higher relative expression level in PAO1 than in PA154197. The black
719 dashed lines represent 4 fold (value of log2 > 2) changes in expression. Genes and operons with
720 distinctive expression patterns in the two strains are indicated. Among them, antibiotic resistance

721 genes are highlighted in red, genes encoding virulence factors are highlighted in green (expressed
722 in a higher level in PA154197 than PAO1) or purple (expressed in a higher level in PAO1 than in
723 PA154197). X-axis represents the gene locus with PAO1 genome as reference.

724 **Figure 4.** Several multidrug efflux pump genes are over-expressed in *P. aeruginosa* PA154197.
725 **A.** RPKM abundance of the major efflux pump genes in PA154197 and PAO1 calculated from the
726 RNA-Seq data. **B.** RT-qPCR analysis of the expression of selective efflux genes and other genes
727 associated with resistance to specific classes of antibiotics. C. Efflux activities of PA154197 and
728 PAO1 measured by ethidium bromide accumulation**.** Higher fluorescence indicates lower efflux
729 activity.

730 **Figure 5.** Virulence and production of several virulence factors in PA154197 and PAO1. **A.**
731 Pyocyanin production in PA154197 and PAO1 cells cultured in both LB broth and agar. **B.**
732 Pyoverdine production examined under UV light. **C.** Biofilm formation examined by the crystal
733 violet stain. **D.** Swimming and swarming motilities examined in the corresponding specific agar
734 plates. **E.** Virulence of PA154197 and PAO1 measured in a *C. elegans* infection model. N2 *C.*
735 *elegans* grown to L4 stage adults were infected with PA154197 or PAO1 for 24hrs. Survival of *C.*
736 *elegans* were monitored under the light microscope and recorded.

737 **Figure 6.** Hyper-activation of the PQS quorum sensing system independent of the master system
738 Las and Rhl in PA154197. **A.** Schematic diagram of the three quorum sensing systems in *P.*
739 *aeruginosa*, Las, Rhl, and PQS, and their selective regulon. Relative expression of the genes in the
740 Las, Rhl, and PQS regulon is depicted in color scheme with the genes expressed at a lower level
741 in PA154197 than in PAO1 in red color and those expressed at a higher level in PA154197 than

in PAO1 in blue color. RPKM abundance of the genes calculated from the RNA-Seq data are indicated. **B.** RT-qPCR of selective genes belonging to the Las, Rhl, and Pqs regulon, respectively.

Figure 7. Schematic model to show the pathoadaptation mechanism adopted by PA154197 to modulate its antibiotic resistance and virulence. In the high virulent, susceptible strains, the three quorum sensing (QS) systems Las, Rhl, and Pqs mediate the production of a variety of virulence factors and a high virulence in the cell. Antibiotic resistant strains with acquired resistance determinants often carry mutations in the master QS regulator Las to downregulate the QS system and virulence. Strains with pathoadaptive strategy such as PA154197 uncouple the activation of the secondary QS system Pqs from Las and Rhl to maintain an uncompromised virulence with simultaneous production of its resistance traits.

753 Table 1 The genomic features of *P. aeruginosa* PA154197.

754

Features	Length (bp)	% GC content	Genes	Proteins	rRNA	tRNA	ncRNA	Pseudo genes	CRISPR arrays
PA154197	6,445,239	66.4%	5,923	5,816	12	65	4	26	3

755

756

757 Table 2. Mutational changes of genes conferring antibiotic resistance and their expression levels in
758 PA154197 relative to that in PAO1.

759

Genes	Non-synonymous/Indel mutations in encoding region	Log2FoldChange (PA154197/PAO1)
mexS	D249-N	1.38
mexT	Del (8bp:237-244),F172-I,G301-C	0.60
mexE	N/A	6.93
mexF	N/A	6.61
oprN	N/A	6.69
mexG	N/A	3.65
mexH	N/A	3.80
mexI	A782-E, A936-T	3.87
opmD	N/A	3.77
armR	S21-T,Y32-C	
mexR	E76-*	2.54
mexA	N/A	3.47
mexB	I1001-T	3.52
oprM	N/A	3.44
mexX	Q4-H,K329-Q,L331V,W358-R	-
mexY	T543-A,L984-F	-
mexZ	N/A	-
mexC	P57-S,R76-Q,H310-R,S330-A,A378-T,P383-S,A384-V	2.05
mexD	T87-S,A155-T,E257-Q,E314-D,V434-A,N669-D,S685-G,I703-V,S845-A,S915-A,I982-V,K1031-	0.72

	R,S1040-T	
oprJ	T376-S,K413-M	-
mexJ	F13-L,A314-P	2.86
mexK	I21-L,K694-R,A841-T	3.16
mexL	S4-P	0.97
muxA	T261-A	-
muxB	N/A	-
muxC	N/A	-
opmB	N/A	-
mexP	N/A	1.03
mexQ	I294-V,V384-I,G505-D,V517-A,R656-K,D722-E	-
opmE	S46-G,I50-V,S175-T,W354-R	-
oprD	D43-N,S57-E,S59-R,E202-Q,I210-A,E230-K,S240-T,N262-T,A267-S,A281-G,K296-Q,Q301-E,R310-G,V359-L,Del(6bp:1132-1137),M372-V,S373-D,D374-S,N375-S,N376-S,V377-S,K380-Y,N381-A,Y382-G,G383-L	
ampC	T105-A	-0.88
ampR	N/A	-
gyrA	T83-I, Del(6bp:2734-2739)	-
gyrB	N/A	-
parC	N/A	-
parE	N/A	0.84
parS	H398R	0.64
parR	N/A	0.61

mvaT	N/A	-0.48
poxB	N/A	-2.55
nalC	G71-E,E153-Q,S209-R	0.42
nalD	N/A	-
aph	A14-S	-
amgS	I260-V,G288-D	-
spuF	P276-S	-
fusA1	I186-V	0.89
fusA2	S176-A,A690-S,G695-A	-2.78

Notes: N/A, no non-synonymous mutation occurred; Ins: insertion; Del: deletion; "-" indicates not significant difference. "*": stop codon.

763 **Figures:**

764 **Figure 1.**

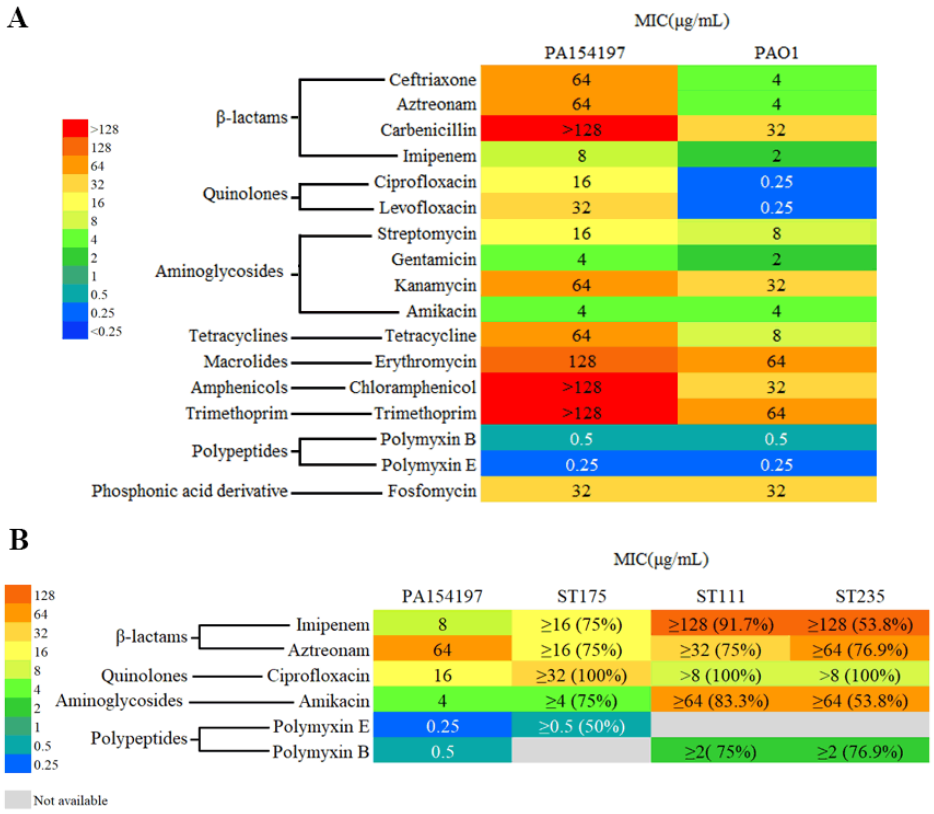

765

766

767 **Figure 2.**

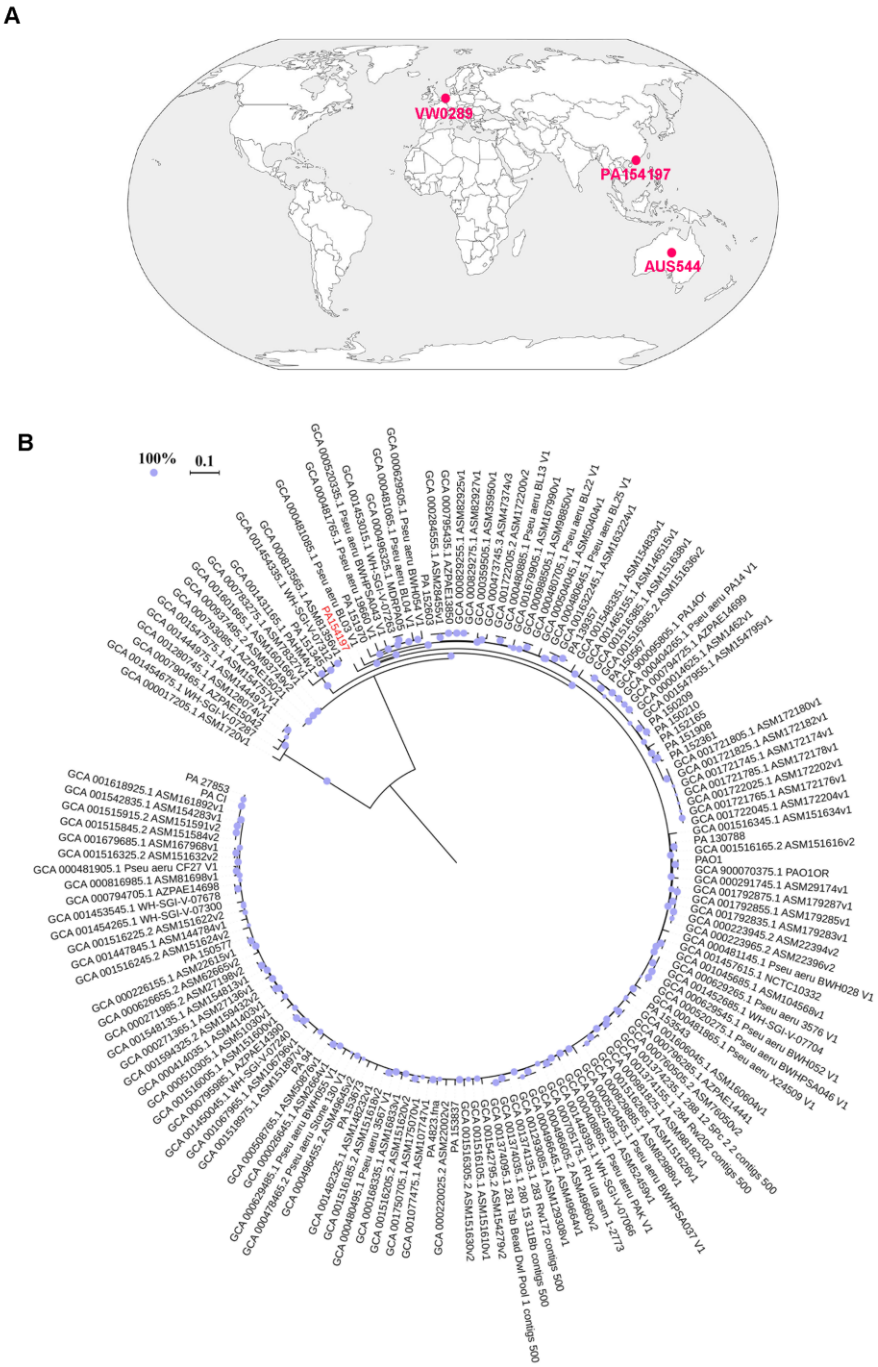

768

769

770 **Figure 3.**

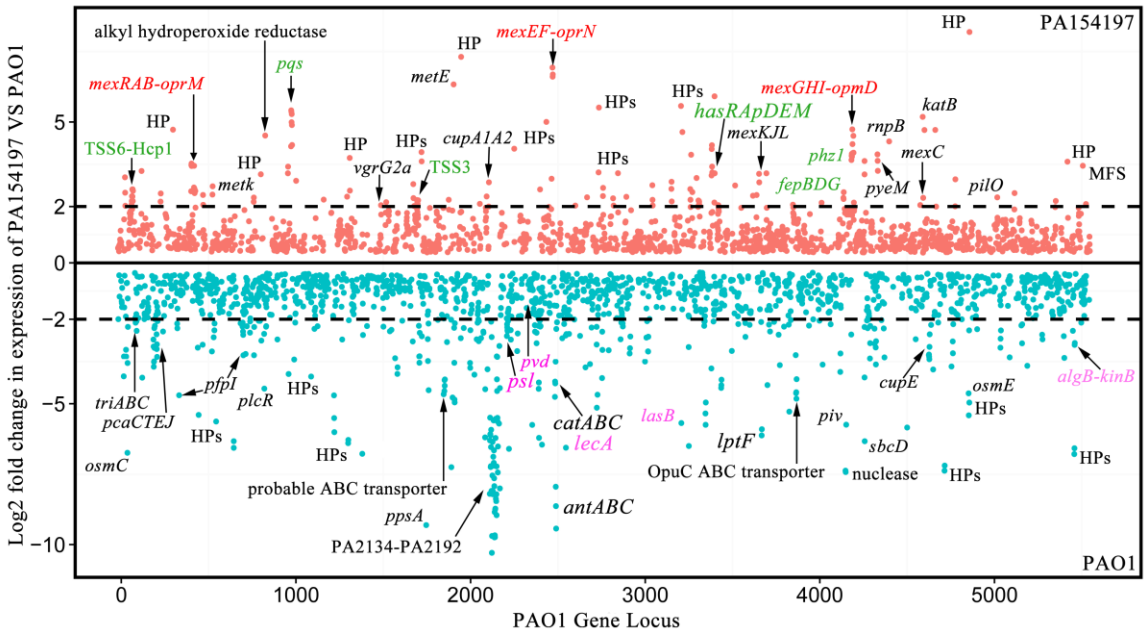

771

772

773 **Figure 4.**

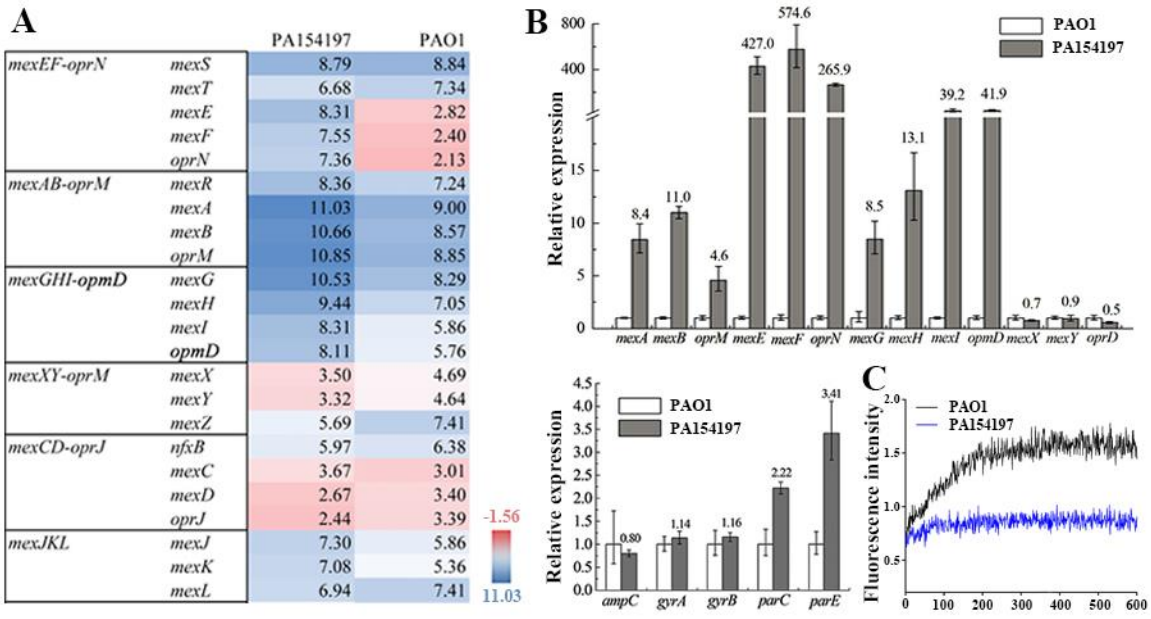

774

775

776 **Figure 5.**

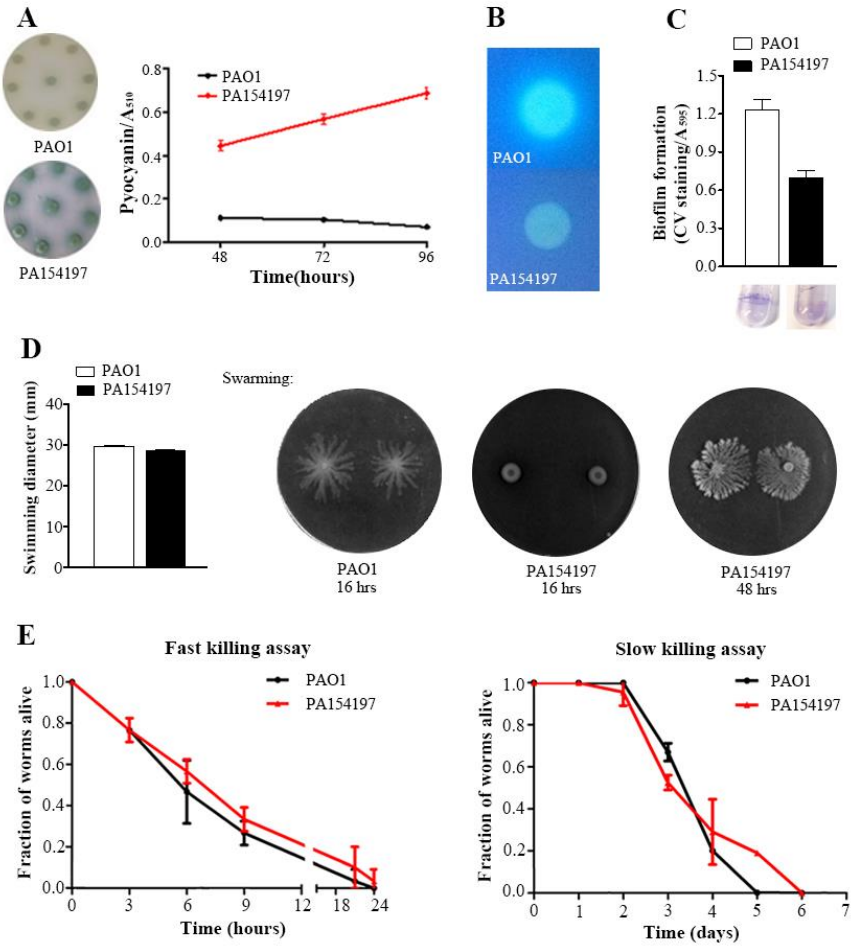

777

778

779

780 **Figure 6.**

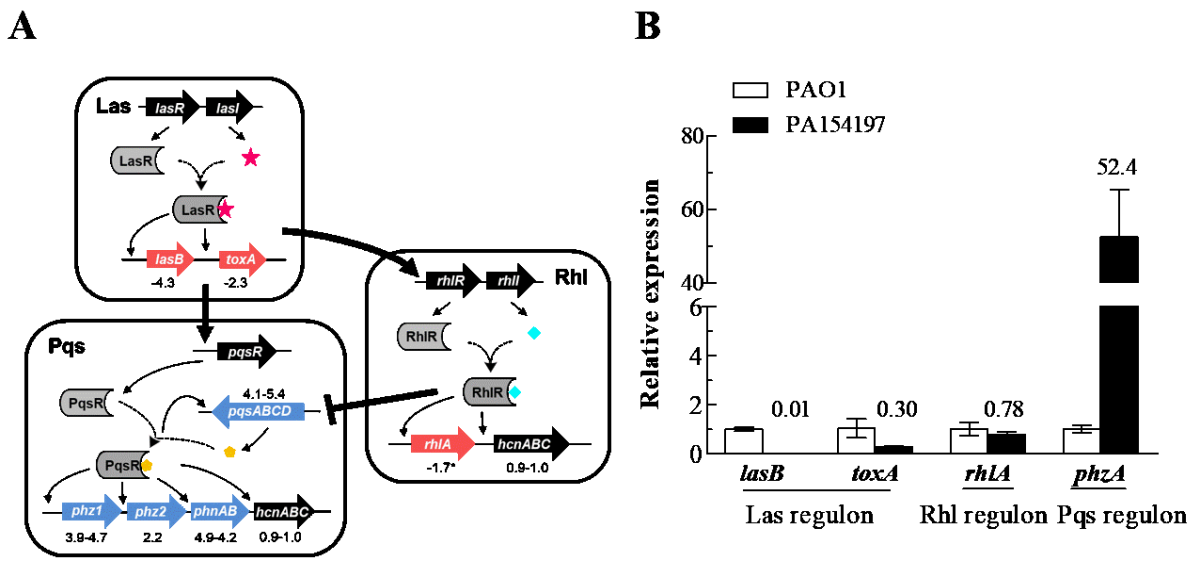

781

782

783 **Figure 7.**

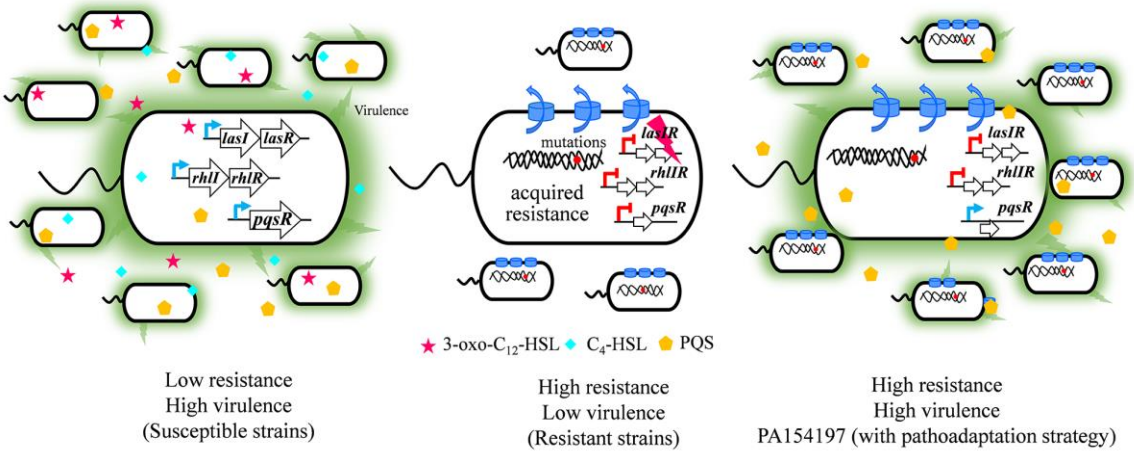

784